ELSEVIER

Journal of Atmospheric and Solar-Terrestrial Physics 66 (2004) 1691–1701

Journal of ATMOSPHERIC AND SOLAR-TERRESTRIAL PHYSICS

www.elsevier.com/locate/jastp

Global scale annual and semi-annual variations of daytime NmF2 in the high solar activity years

Tao Yu[a,b,*], Weixing Wan[a], Libo Liu[a], Biqiang Zhao[a]

[a]*Institute of Geology and Geophysics, CAS, Beijing 100029, China*
[b]*National Satellite Meteorological Center, CMA, Beijing 100081, China*

Received 18 April 2002; received in revised form 28 November 2002; accepted 26 September 2003

Abstract

The annual and semi-annual variations of the ionosphere are investigated in the present paper by using the daytime F2 layer peak electron concentration (NmF2) observed at a global ionosonde network with 104 stations. The main features are outlined as follows. (1) The annual variations are most pronounced at magnetic latitudes of 40–60° in both hemispheres, and usually manifest as winter anomalies; Below magnetic latitude of 40° as well as in the tropical region they are much weaker and winter anomalies that are not obvious. (2) The semi-annual variations, which are usually peak in March or April in most regions, are generally weak in the near-pole regions and strong in the far-pole regions of both hemispheres. (3) Compared with their annual components, the semi-annual variations in the tropical region are more significant.

In order to explain the above results, we particularly analyze the global atomic/molecular ratio of [O/N2] at the F2 layer peak height by the MSIS90 model. The results show that the annual variation of [O/N2] is closely related with that of NmF2 prevailing in mid-latitudes and [O/N2] annual variation usually may lead to the winter anomalies of NmF2 occurring in the near-pole region. Moreover, NmF2 semi-annual variations appearing in the tropical region also have a close relationship with the variation of [O/N2]. On the other hand, the semi-annual variations of NmF2 in the far-pole region cannot be simply explained by that of [O/N2], but the variation of the solar zenith angle may also have a significant contribution.

Keywords: Ionospheric annual and semi-annual variation; Winter anomaly; Atomic/molecular ratio

1. Introduction

As expected by Chapman theory of ionization, the electron concentrations should vary regularly with solar zenith angles, as it does in the well-known 'Chapman layer'. Therefore, any departure from the 'solar-controlled' behavior in the ionosphere is originally considered as 'anomaly'. In fact, the F2 layer is 'anomalous' rather than simply controlled by the solar zenith angle according to the prediction of Chapman theory. There are many well-known 'anomalies' in the F2 layer, such as the 'winter anomaly', 'seasonal anomaly', and 'semi-annual anomaly' (Rishbeth, 1998, 2000b; Rishbeth and Mendillo, 2001; Wills et al., 1994). Since first reported by Appleton and Naismith (1935), a variety of anomalies have become very prominent and many authors have begun to study these interesting phenom-

*Corresponding author.
E-mail address: yutao@nsmc.cma.gov.cn (T. Yu).

1364-6826/$ - see front matter © 2004 Elsevier Ltd. All rights reserved.
doi:10.1016/j.jastp.2003.09.018

ena. Yonezawa and Arima (1959) and Yonezawa (1971) scrutinized the relationships between the winter anomaly, the annual anomaly, and the semi-annual anomaly at mid-low latitudes with the solar activity and geomagnetic latitude. Torr and Torr (1973) constructed maps with observed foF2 data to show the global distributions of these anomalies mentioned above. Balan et al. (1998) studied the annual variations in the ionosphere and thermosphere during solar maximum period by using the Japanese MU radar data, and later, they gave a brief review on the annual variation (Balan et al., 2000). Historical details on this topic were well presented by Rishbeth (1998, 2000b).

Many theories have been proposed to explain the variations of the F2 layer anomalies, such as the 'Geometrical explanations' (Yonezawa and Arima, 1959), the 'Thermal explanations' (Appleton, 1935) and the 'Chemical explanations' (Rishbeth and Setty, 1961; Wright, 1963). Among them, the 'Chemical explanations' was proved to be rather reasonable and has been accepted in some extent. Rishbeth and Setty (1961) and Wright (1963) recognized that the change of chemical compositions in the upper atmosphere, such as the atomic–molecular ratio [O/N2], could mainly account for the variation of NmF2 in daytime. Subsequently, Johnson (1964) and King (1964) suggested that the thermospheric circulation from the summer hemisphere to the winter one could affect the [O/N2] ratio and finally change the NmF2.

Recently, numerical methods have been applied to investigate the electron density variations in the ionosphere. Based on the global thermospheric circulation theory, Fuller-Rowell and Rees (1983) reproduced the seasonal variation of NmF2. After considering the offset of the geographic and geomagnetic poles, Millward et al. (1996) tried to explain the longitude differences in seasonal and semi-annual characteristics at mid-latitudes. Fuller-Rowell (1998) proposed a mechanism named 'thermospheric spoon' to interpret the semi-annual variation in the ionosphere. With a coupled thermosphere–ionosphere–plasmasphere model (CTIP), Zou et al. (2000) re-examined the global thermospheric circulation theory and how far the semi-annual anomaly could be explained by this theory without invoking other causes. Thereafter, Rishbeth et al. (2000a) gave a detailed physical discussion.

In this paper, we use the global ionosonde data in six high solar activity years (1958, 1959, 1979–1981 and 1989) to analyze the annual and semi-annual variations of the noon NmF2. First, we introduce a regression technique to yield the annual and semi-annual components from the original data. Then, these components are used to construct global distribution maps and their main features are outlined. Finally, we particularly discuss how far the phenomena concerned can or cannot be explained by existing theories.

2. Analysis method and example

The ionosonde data taken from the NOAA CD-Roms cover more than 100 global stations and span from 1958 to 1989. In order to study the annual and semi-annual variations of NmF2 in high solar activity years, we select the foF2 data in the years of 1958 (yearly average $\overline{F107} = 228.7$), 1959 (205.8), 1979 (191.6), 1980 (197.8), 1981 (203.2) and 1989 (213.4), which are taken as high solar activity years by Rishbeth and Mendillo (2001). Since we concern about only the phenomena at mid-latitudes and in tropical regions, we exclude the data at polar stations. We also remove the stations when their data are too scarce during the selected years. Thus, data are collected from 104 stations all over the world. Locations of each station are shown in Figs. 2 and 5.

We take foF2 at 14:00LT as the sample for daytime foF2. First, the measured foF2 is converted into NmF2, and then we express the NmF2 in three terms, which represent the average value, the annual and semi-annual components, as follows:

$$NmF2(d) = \{NmF2\}_0 + \{NmF2\}_1 + \{NmF2\}_2 = A_0 + A_1 \cos\frac{2\pi}{T}(d - D1) + A_2 \cos\frac{4\pi}{T}(d - D_2). \quad (1)$$

Here d is day number and T ($T = 365.25$) is total days of a year. A_0 is the yearly average value of the NmF2. A_1 and A_2 are the amplitudes of the NmF2 annual and semi-annual components. D_1 and D_2 are the corresponding phases and denote the days in which the maximum NmF2 appears.

As an example of the above expression, the NmF2 at Canberra Station (149.1°, −35.3°) and its components regressed by Eq. (1) are shown in Fig. 1. Since NmF2 itself has a strong day-to-day variation (Forbes et al., 2000; Rishbeth and Mendillo, 2001), the observed data (denoted as circles) scatter from the regression result (bold solid line). We included the storm-time data because they have no significant influence on the final regression result.

In Fig. 1, the four vertical lines denote March equinox, June solstice, September equinox and December solstice, respectively. The horizontal dotted line denotes yearly average of NmF2. The dashed line denotes NmF2 annual component with amplitude (A_1) of $4.8 \times 10^{11}\,m^{-3}$ and phase (D_1) of 162.6 days. So the annual variation reaches its peak roughly 10 days before June solstice, and there is an obvious winter anomaly for NmF2 over Canberra Station, which is similar to the previous work (Yonezawa, 1971; Torr and Torr, 1973; Zou et al., 2000). Moreover, the thin solid line denotes the semi-annual component with amplitude (A_2) of $2.9 \times 10^{11}\,m^{-3}$ and phase (D_2) of 105.7 days. Therefore,

the daytime NmF2 over Canberra has a dominant annual variation and a considerable semi-annual variation.

3. Results

3.1. Annual variation

In the following global maps (Figs. 2, 5 and 9), we mark circles on the location of the station. The radii of the circles denote the normalized annual amplitude (A_1/A_0). The plus sign '+' and the cross '×' show different phase information: '×' represents the NmF2 annual variation peak closer to June solstice and '+' represents that peak closer to December solstice. Therefore, both the '+' phase in the northern hemisphere and the '×' phase in the southern hemisphere denote winter anomaly.

The global distribution of NmF2 annual variation in the high solar activity years is shown in Fig. 2. The dotted curves represent the isomagnetic latitudes from −80° to 80° with a step of 20° and asterisks are marked in the northern and southern magnetic poles. From Fig. 2, it may be seen that the circles in the northern mid-latitudes regions (magnetic latitudes of 40–60°) are slightly larger than those in other regions. Moreover, the '+' phase is predominant in the whole northern hemisphere. Thus, the NmF2 annual variation is prone to reach its peak at the December solstice. Whereas in the southern hemisphere, the '×' phase, which indicates winter anomaly, is found in the near-pole region (the region near the geomagnetic pole, Rishbeth, 1998), and the '+' phase is predominant in the rest of the region. Another perceivable feature in Fig. 2 is that the amplitudes of annual variation are much larger in the near-pole regions (North America and Australia) than in the far-pole regions (the region far from the geomagnetic pole, such as Far East and South America) and even in Europe and Southern Africa. In addition, although the annual amplitudes are very small at most stations in South America and Southern Africa, at Trelew (−43.2°, 294.7°), the annual variation are much greater than those of the other stations nearby. Finally,

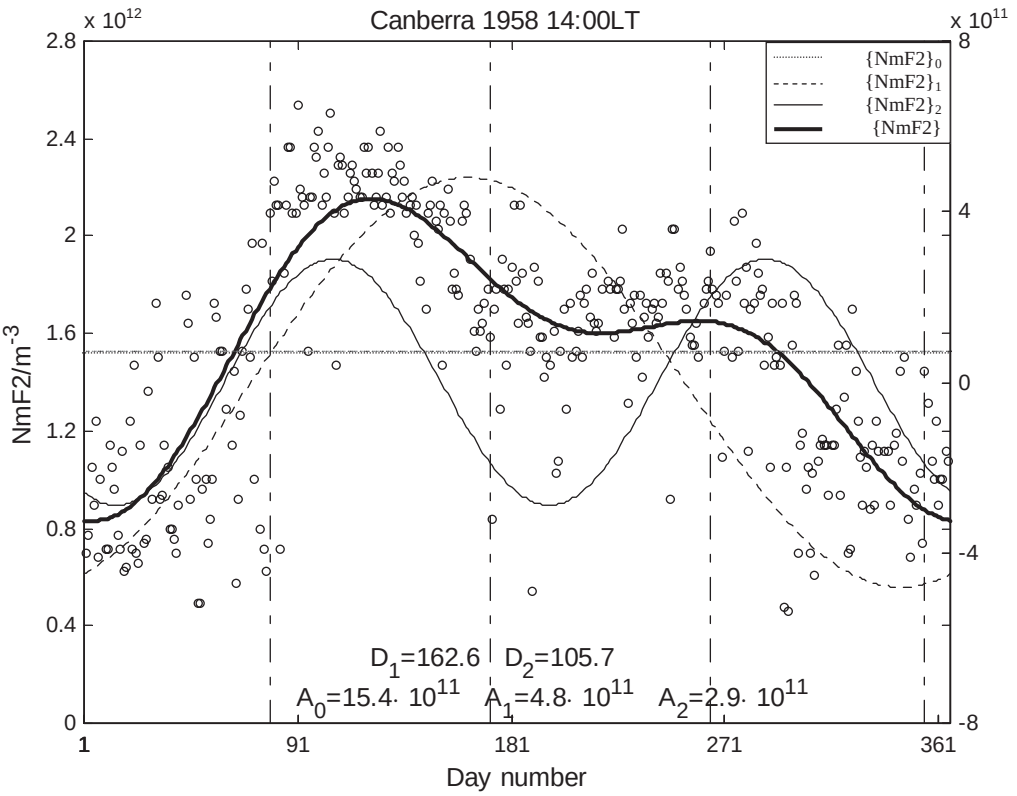

Fig. 1. The daytime (14:00LT) measured NmF2 (circles) and the regression results (bold solid line) at Canberra Station in 1958. The four vertical dash lines denote vernal equinox, summer solstice, autumnal equinox and winter solstice in northern hemisphere respectively. The horizontal dotted line denotes the value of $NmF2_0$ indicating yearly average of NmF2. The dashed line denotes the value of $NmF2_1$ representing the NmF2 annual component. The thin solid line denotes the value of $NmF2_2$ representing the semi-annual component. The coefficients in Eq. (1) are shown in the bottom of this figure

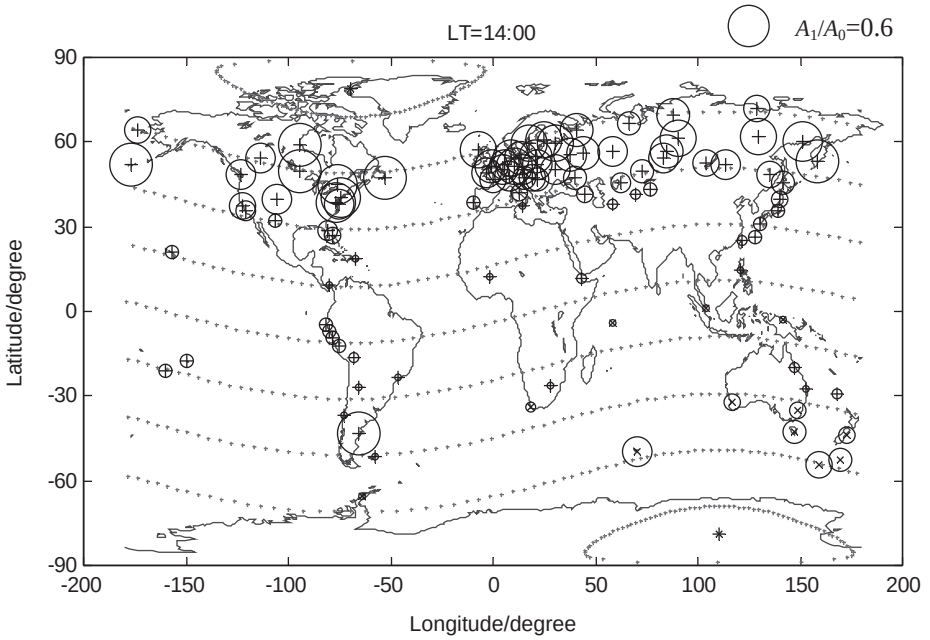

Fig. 2. The global distributions map for the daytime NmF2 annual amplitudes. The radius denotes the normalized annual amplitude (A_1/A_0), and the '+' implies that the NmF2 annual variation reaches its peak in the days closer to December solstice. The cross '×' denotes that it is opposite to what the plus sign '+' does.

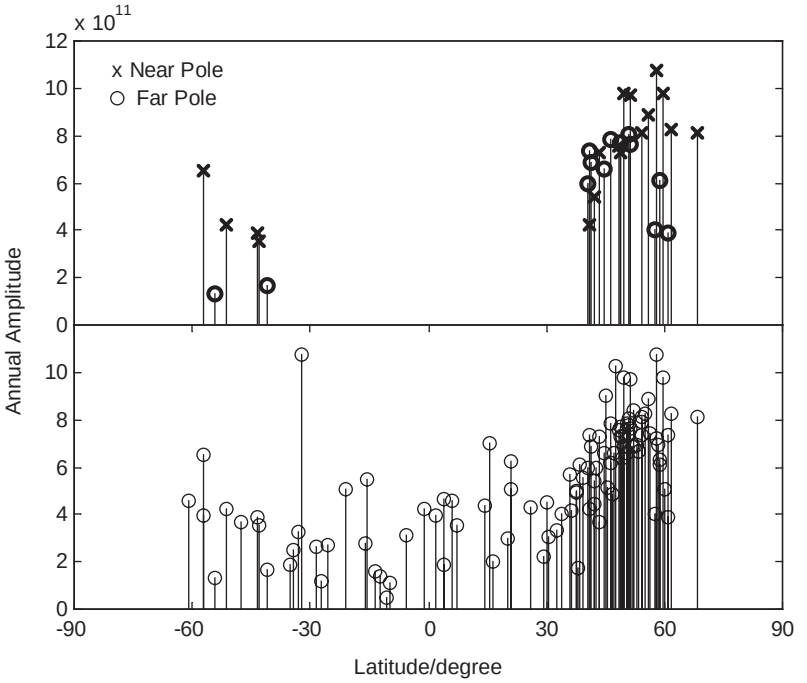

Fig. 3. The annual amplitude for the daytime NmF2 variation plot against the magnetic latitude. In the top panel we plot stations in the far-pole (o) and near-pole (x) region, respectively. In the bottom panel we plot the global stations.

we may also notice that the annual amplitudes in the tropical region are much smaller than those in other regions.

Fig. 3 shows the NmF2 annual component versus magnetic latitude. In the top panel, we give the annual amplitudes for the near-pole stations ('×') and the

far-pole stations ('O'). It is obvious from Fig. 3 that the annual amplitudes are large in mid-latitude and small in lower latitude and they are obviously reducing with decreasing latitude. As global average, the annual amplitudes in the northern hemisphere are generally larger than those in the southern hemisphere. In

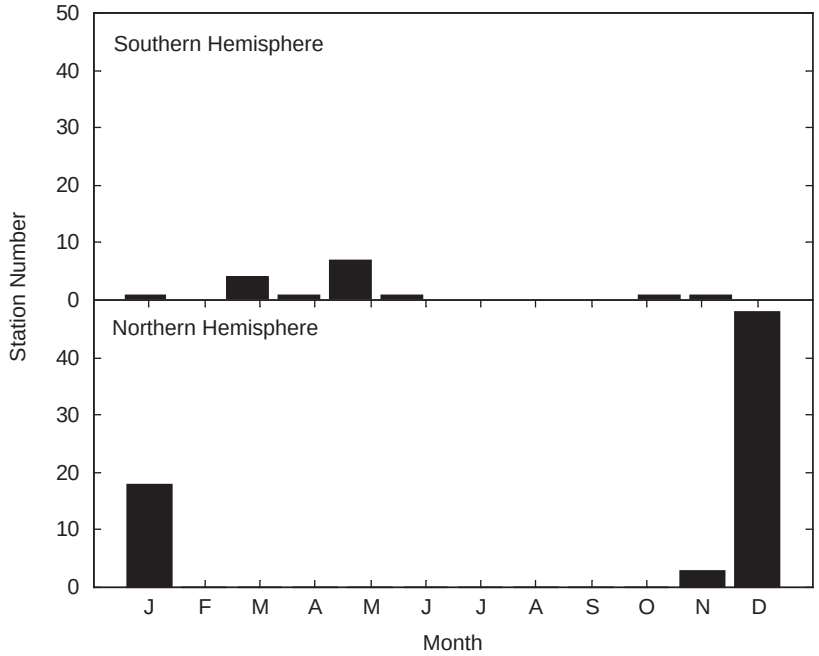

Fig. 4. The phase of NmF2 annual component measured in the southern hemisphere (top panel) and the northern hemisphere (bottom panel). The horizontal axis denotes the months from January to December, and the vertical axis indicates the number of stations at which NmF2 annual component peaks in respective months.

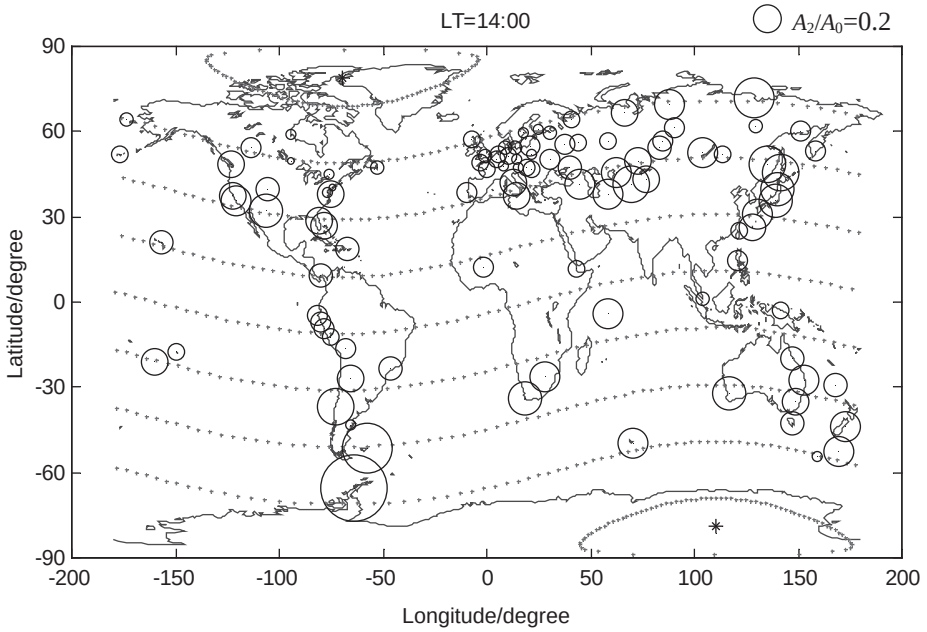

Fig. 5. The global distribution map for the daytime NmF2 semi-annual amplitude., The radius denotes the normalized semi-annual amplitude (A_2/A_0) of the NmF2. There are small dots in every circle that represent the position of the stations.

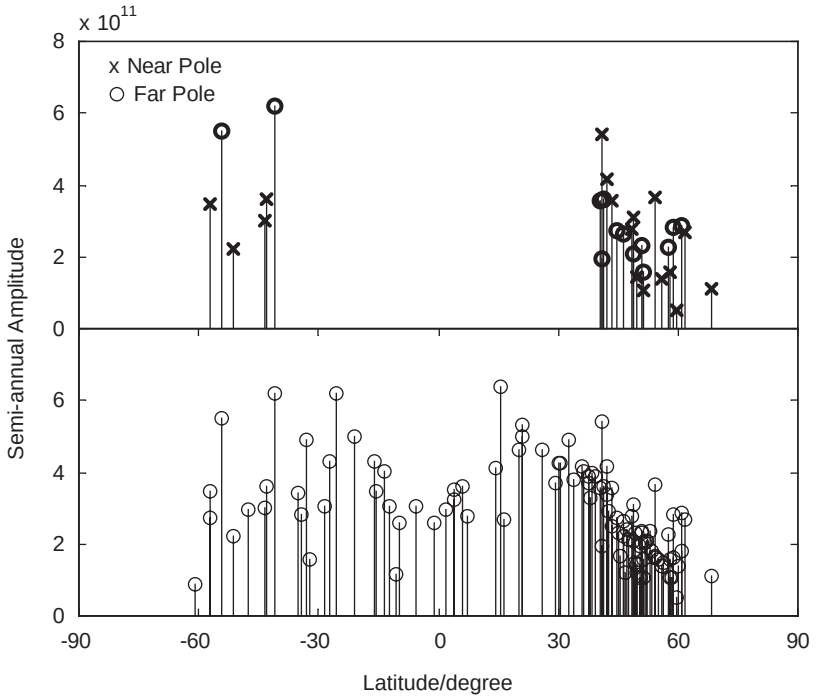

Fig. 6. The semi-annual amplitude for the daytime NmF2 variation plot against the magnetic latitude. In the top panel we plot stations in the far-pole (o) and near-pole (x) region, respectively. In the bottom panel we plot the global stations.

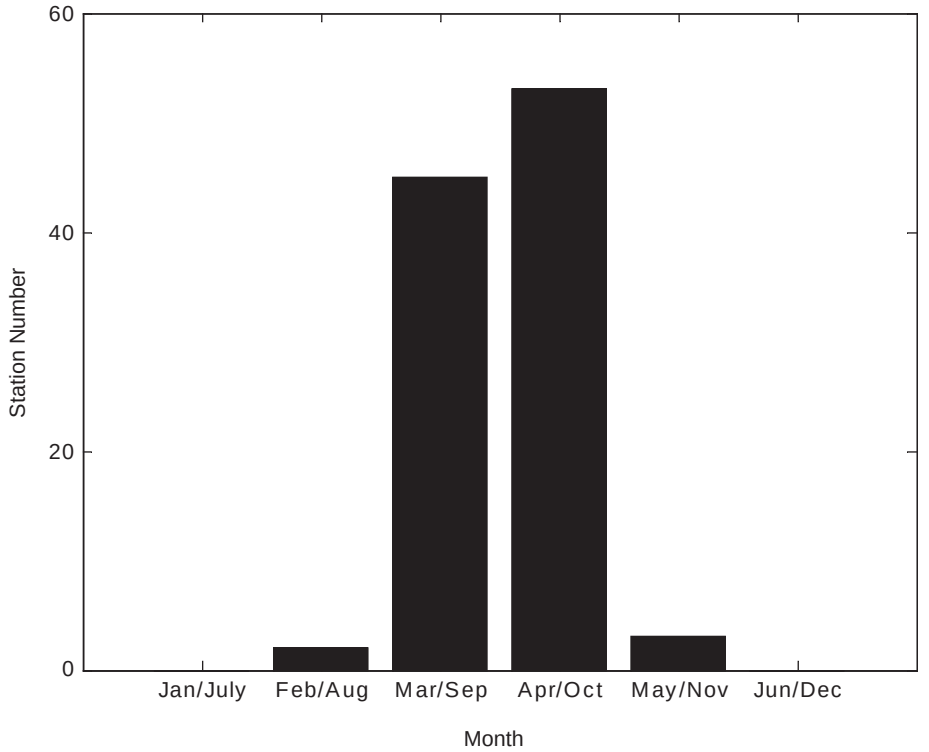

Fig. 7. The phase of the global NmF2 semi-annual component. The horizontal axis denotes the months from January to June, and the vertical axis indicates the number of stations at which the NmF2 semi-annual component peaks in respective months.

addition, another important feature from this figure is that the annual amplitudes are larger in the near-pole region than those in the far-pole region.

The phases for NmF2 annual component are statistically analyzed and shown in Fig. 4. In the top and bottom panels, we, respectively, display the results of southern stations and northern stations. The statistical result reveals that most stations in the northern hemisphere reach their annual variations peak in December (48 stations) and January (19 stations), a small amount of stations peak in November (3 stations) and no station reaches annual variations maximum in the remaining months. So it seems that almost all the stations in the northern hemisphere have obvious winter anomaly. On the other hand, it is also obvious that most stations in southern hemisphere peak in March and May and very few stations peak in January, April, June, October and November. Therefore, it is understood that, in the southern hemisphere, most stations have winter anomaly and very few stations do not. In the end, it can also be concluded from Fig. 4 that there is an annual or non-seasonal anomaly in the global ionosphere (Rishbeth, 1998), for which, taking the world as a whole, the NmF2 appears to be greater in December than in June.

3.2. Semi-annual variation

The global distribution maps for the mean semi-annual component are shown in Fig. 5. It is noticeable that the semi-annual amplitudes are large at most far-pole stations (Southern American and far east) and small in the near-pole regions (North American, Australia and west Europe). In the tropical regions, the semi-annual amplitudes are also significantly large comparing to their annual component amplitudes shown in Fig. 2.

The latitudinal variations of the semi-annual components are illustrated in Fig. 6. In the top panel we respectively plot the semi-annual amplitudes for the stations in the far-pole ('O') and near-pole (' × ') regions, and in the bottom panel we plot the amplitudes for the global stations. The results show that the semi-annual amplitudes usually distribute as a double hump, which are large in mid-latitude and a little smaller at the equator and very small in high latitudes and these amplitudes are of nearly comparable magnitudes in both hemispheres. Moreover, the semi-annual amplitudes of NmF2 in the northern hemisphere and southern hemisphere are symmetric with the magnetic equator. Additionally, in the southern hemisphere, the semi-annual amplitudes in the far-pole region are much larger than those in the near-pole region, whereas, in the northern hemisphere, the semi-annual amplitudes are nearly equivalent both in the far and near-pole regions.

The histogram for the phases of semi-annual component is shown in Fig. 7. The horizontal axis denotes the

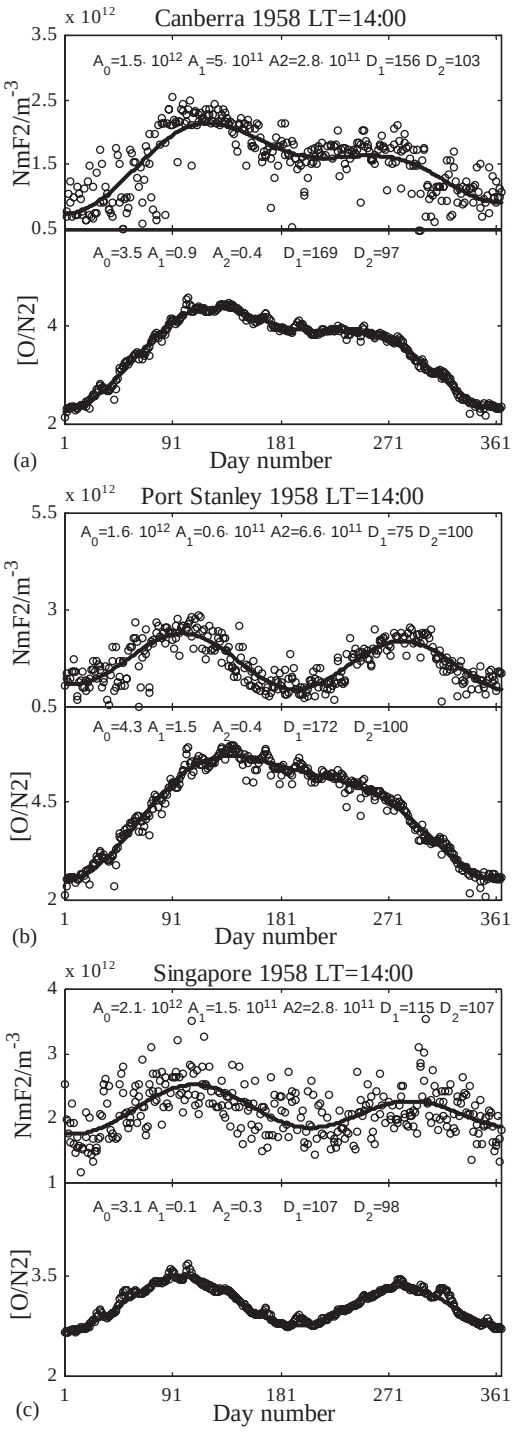

Fig. 8. The variation for the daytime NmF2 at Canberra Station, Port Stanley Station and Singapore Station are respectively, shown in the upper panel of 8(a)–(c), and the [O/N2] at those stations are shown in the bottom panel.

Table 1
The annual and semi-annual amplitudes (normalized) and phases for NmF2 and [O/N2] at the example stations

Station	Region	Parameter	A_1/A_0	D_1	A_2/A_0	D_2
Canberra	Near-pole	NmF2	0.33	156	0.19	103
		[O/N2]	0.26	169	0.11	97
Port Stanley	Far-pole	NmF2	0.04	75	0.41	100
		[O/N2]	0.34	172	0.09	100
Singapore	Tropical	NmF2	0.07	115	0.13	107
		[O/N2]	0.03	107	0.10	98

months, and the vertical axis denotes the station numbers. Since the period of semi-annual variation is 6 months, its phase ranges from January/July to June/December. From this figure, we find that nearly all the global stations reach their semi-annual peaks in March/September (45 stations) and April/October (53 stations), very few stations peak in February/August and May/November and no stations peak in January/July and June/December.

4. Discussion and physical explanation

Many authors proposed assumptions to explain the annual and semi-annual ionospheric variations. Among them, Rishbeth and Setty (1961) and Wright (1963) suggested that a change in the ratio of atomic oxygen concentration to molecular nitrogen ([O/N2]) in the upper atmosphere might account for the daytime NmF2 variation. Later, Johnson (1964) and King (1964) figured out that the thermospheric circulation from the summer hemisphere to the winter one could change the [O/N2] and lead to the variation of NmF2. In the daytime, the F2 layer is usually in 'quasi-equilibrium' state, the production q and loss terms β are roughly in balance. Here q depends mainly on [O] and β depends mostly on $[N_2]$ with some contribution from molecular oxygen $[O_2]$. Now ignoring the contribution from $[O_2]$, the peak electron concentration in the steady state is given by

$$[N_e] \sim q/\beta \propto [O/N_2]. \quad (2)$$

Therefore, the daytime NmF2 is approximately proportional to [O/N2] at the peak height.

In the following section, we try to investigate to what degree the annual variation of NmF2 at mid-latitudes (illustrated in Fig. 2) and the semi-annual variation, both in the far-pole region and the tropical region (Fig. 5), can be explained by the above theory. As examples, we select the near-pole station, Canberra (149.1°, −35.3°), the far-pole station, Port Stanley (−57.8°, −51.7°) and the tropical station, Singapore (103.8°, 1.3°), to compare their observed NmF2 with [O/N2] at 300 km altitude (usually the daytime F2 peak height) calculated from the empirical model MSIS90 (Hedin, 1991). Fig. 8 shows the variations of [O/N2] and NmF2 at the three stations. In the figure, the circles represent the observed NmF2 or the calculated [O/N2] and the bold solid lines denote the corresponding variation regressed by Eq. (1). The yearly average value (A_0), the amplitudes and phases for annual and semi-annual variations (A_1, A_2, D_1, D_2) are presented on the top of Figs. 8a–c and also shown in Table 1. From Fig. 8 and Table 1 we can find that (1) At Canberra Station, the amplitudes and phases of annual and semi-annual components for both NmF2 and [O/N2] are nearly approximate to each other and both of them have a strong annual component and a weak semi-annual component. (2) At Port Stanley Station, all the amplitudes and phases of NmF2 and [O/N2] are quite different except for their semi-annual component phases. The variations of NmF2 and [O/N2] are quite different that NmF2 has a pronounced semi-annual component while [O/N2] has a noticeable annual component. (3) At Singapore Station, NmF2 and [O/N2] have similar value both in their semi-annual amplitudes and phases, while they have different value in their annual amplitudes. Therefore the variations of NmF2 and [O/N2] are very similar to each other and both of them vary in a semi-annual pattern, reaching their peak in April and October.

According to Fig. 8 and Table 1, we may draw a brief conclusion. At the near-pole station Canberra, NmF2 varies in the same pattern as [O/N2] does, so we suggest that the NmF2 should be prominently controlled by [O/N2]. At the far-pole station Port Stanley, NmF2 has a dominant annual variation while [O/N2] has a semi-annual one. So we assume that the variation of NmF2 should be partly controlled by the [O/N2]. At the tropical station Singapore, both NmF2 and [O/N2] have a dominant semi-annual variation, but their annual components do not fit so well. So besides [O/N2], some other mechanisms may contribute to NmF2 variation.

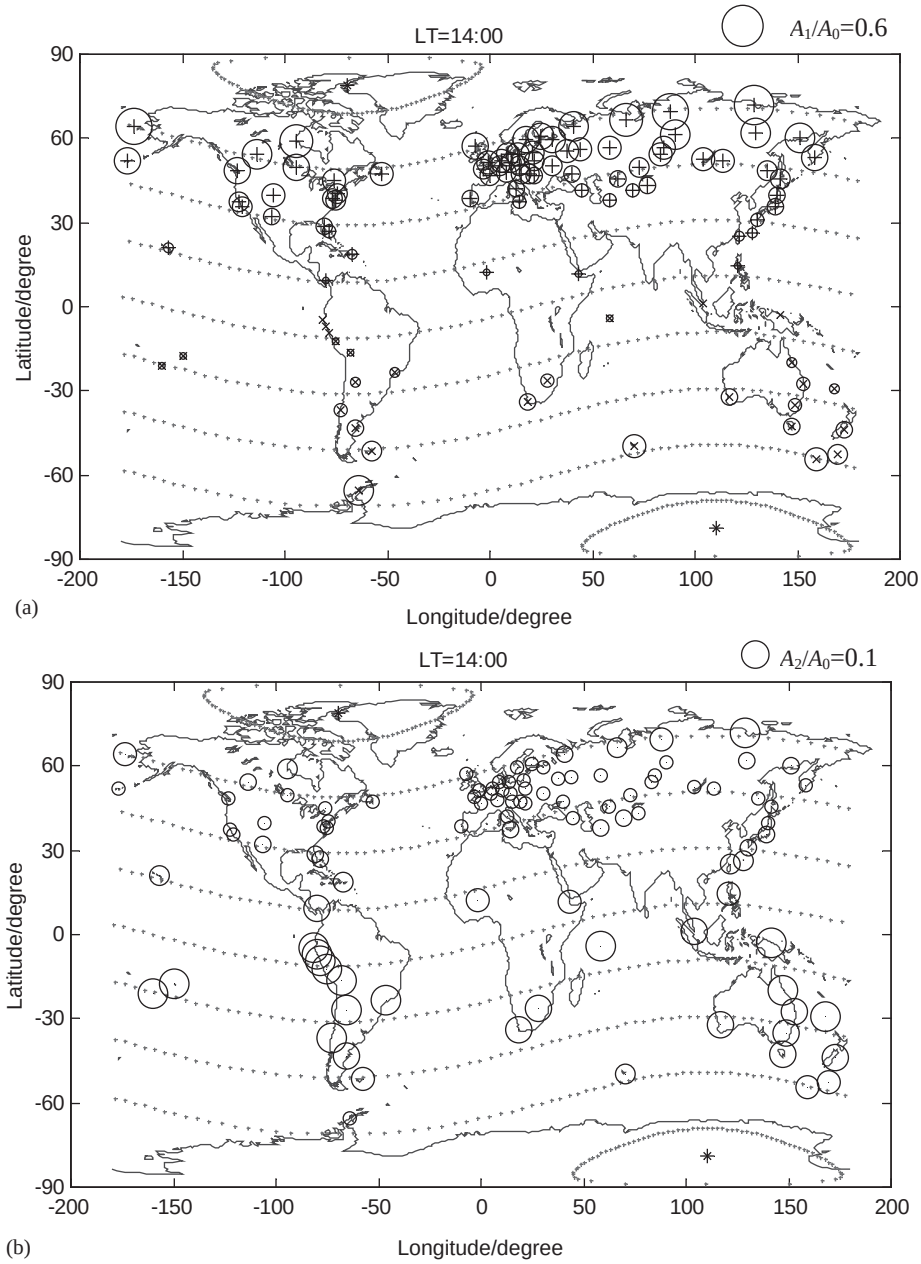

Fig. 9. The global distribution maps for the daytime [O/N2] annual and semi-annual component are shown in Fig. 9(a) and (b), and the radius denotes the normalized annual amplitude (A_1/A_0) and semi-annual amplitude (A_2/A_0). The plus '+' in the upper panel implies that the [O/N2] annual variation reaches its peak in the days closer to the December solstice. The cross '×' denotes that it is opposite to what the plus sign '+' does.

In order to study how far the change of [O/N2] may contribute to NmF2 variation in different regions, we calculated the daytime [O/N2] at 300 km from the empirical model MSIS90 in the stations as shown in Fig. 2. The calculated data are also treated with the regression of Eq. (1) to obtain the amplitude and phase of their annual and semi-annual components. To compare with the results in Fig. 2, we draw a global distribution map for [O/N2] annual and semi-annual variations as shown in Fig. 9 and discuss them as following.

(1) Near-pole region. It may be seen from Fig. 9a that there are pronounced [O/N2] annual variations in the near-pole regions of both hemispheres, i.e. North America and Australia. Their phases indicate these annual variations all are winter anomalies. Similar as illustrated in Fig. 2, the annual amplitudes of NmF2 are also large and manifest as winter anomaly in the near-pole regions. Moreover, Fig. 9b shows that the semi-annual components are very small in North America and slightly large in Australia. Similarly, the NmF2 semi-annual amplitudes in Fig. 5 are also very small in North America and a little large in Australia. These phenomena are in accordance with the case of Canberra Station. Therefore, we may conclude that in the near-pole regions, the change of [O/N2] could mainly contribute to the NmF2 annual variation.

(2) Far-pole region. Fig. 9a also shows that in the far-pole regions, the [O/N2] variation has a considerable large annual component with evident winter anomaly, while Fig. 2 reveals that NmF2 variation has very small annual component and no winter anomaly in South America. At the same time, Fig. 9b shows that the semi-annual component of [O/N2] is very large in South America and small in far east, while Fig. 5 reveals the semi-annual component of NmF2 is considerably large in those regions. These differences imply that NmF2 does not behave as [O/N2] does in the far-pole regions. Thus NmF2 may be controlled not only by [O/N2], but also by some others. Such as the mechanism proposed by Millward et al. (1996), Balan et al. (1998) and Fuller-Rowell (1998), which combined the change of [O/N2], solar zenith angle and thermospheric circulation, can explain well the dominant semi-annual variation of NmF2 in the far-pole region.

(3) Tropical region. It is clear from Fig. 9a that the annual component of [O/N2] is very small in the tropical region, so does NmF2 (Fig. 2). Furthermore, from Figs. 9b and 5, the semi-annual components of both [O/N2] and NmF2 are of considerable magnitude. So we suggest that [O/N2] is the main contributor to NmF2 variation in this region.

5. Conclusions

In this paper, the observed daytime NmF2 data over 100 global stations in six high solar activity years (1958, 1959, 1979–1981 and 1989) have been studied to explore the annual and semi-annual behavior of NmF2. The major results are briefly recapitulated as follows:

(1) The annual variations of NmF2 have noticeable regional characteristics. As a global average, the annual amplitudes are large in the northern hemisphere, slightly small in the southern hemisphere, and very small in the tropical region, and they are much larger in the near-pole regions than in the far-pole regions. In addition, the winter anomaly is prevailing at mid-latitudes except in South America.

(2) The semi-annual variations of NmF2 also appear to have obvious regional characteristics. The semi-annual variations are very weak in near-pole regions and considerably large in far-pole regions as well as tropical region. Moreover, the semi-annual variations usually reach their peaks in March/September and April/October.

We also investigate the relationship between observed NmF2 and model [O/N2]. The results reveal that, both NmF2 and [O/N2] at near-pole stations have a large annual component with pronounced winter anomaly, so the variation of [O/N2] may mainly contributed to that of NmF2 in this region. At the tropical stations, both NmF2 and [O/N2] vary with a dominant semi-annual pattern, so [O/N2] also be considered as one important contributor to NmF2 semi-annual variation. It is difficult to explain why NmF2 have the pronounced semi-annual variation at far-pole stations, whilst [O/N2] still have noticeable annual variation. We assume that the far-pole NmF2 may be controlled not only by [O/N2], but also by other factors, such as the variation of solar zenith angle.

Acknowledgements

This work was supported by the KIP Pilot Project (kzcx3-sw-144) of CAS, the NNSFC (40134020) and the NKBRSF (G2000078407) in China. The authors would like to acknowledge NOAA and WDC-A for Solar Terrestrial Physics for supplying the worldwide vertical incidence parameter CD-ROM.

References

Appleton, E.V., Naismith, R., 1935. Some further measurements of upper atmosphereic ionization. Proceedings of the Royal Society of London A 150, 685–708.

Balan, N., Otsuka, Y., Bailey, G.J., Fukao, S., 1998. Equinoctial asymmertries in the ionosphere and thermosphere observed by the MU radar. Journal of Geophysical Research 103, 9481–9495.

Balan, N., Otsuka, Y., Bailey, G.J., Fukao, S., Abdu, M.A., 2000. Annual variations of the ionosphere: A review based on the MU radar observations. Advance in Space Research 25, 153–162.

Forbes, J.M., Palo, S.E., Zhang, X., 2000. Variability of the ionosphere. Journal of Atmospheric and Solar-Terrestrial Physics 62, 685–693.

Fuller-Rowell, T.J., Rees, D., 1983. Derivation of a conservation equation for mean molecular weight for a two-constituent gas within a three-dimensional, time-dependent model of the thermosphere. Planet Space Science 31, 1209–1222.

Fuller-Rowell, T.J., 1998. The 'Thermospheric spoon': a mechanism for the semi-annual density variation. Journal of Geophysical Research 103, 3951–3956.

Hedin, A.E., 1991. Extension of the MSIS thermospheric model into the middle and lower atmosphere. Journal of Geophysical Research 96, 1159–1172.

Johnson, F.S., 1964. Composition changes in the upper atmosphere. In: Thrane, E. (Ed.), Electron Density Distributions in the Ionosphere and Exosphere. North-Holland, Amsterdam, pp. 81–84.

King, G.A.M., 1964. The dissociation of oxygen and high level circulation in the atmosphere. Journal of Atmospheric and Solar-Terrestrial Physics 21, 231–237.

Millward, G.H., Rishbeth, H., Fuller-Rowell, T.J., Aylward, A.D., Quegan, S., Moffet, R.J., 1996. Ionospheric F2 layer seasonal and semi-annual variations. Journal of Geophysical Research 101, 5149–5156.

Rishbeth, H., Setty, C.S.G.K., 1961. The F-layer at sunrise. Journal of Atmospheric and Solar-Terrestrial Physics 21, 263–276.

Rishbeth, H., 1998. How the thermospheric circulation affects the ionosphere F2-layer. Journal of Atmospheric and Solar-Terrestrial Physics 60, 1385–1402.

Rishbeth, H., Muller-Wodarg, I.C.F., Zou, L., Fuller-Rowell, T.J., Millward, G.H., Moffett, R.J., Idenden, D.W., Aylwardm, A.D., 2000a. Annual and semiannual variations in the ionospheric F2-layer: II. Physical discussion. Annales Geophysicae 18, 945–956.

Rishbeth, H., 2000b. The equatorial F-layer: progress and puzzles. Annales Geophysicae 18, 730–739.

Rishbeth, H., Mendillo, M., 2001. Patterns of F2-layer variability. Journal of Atmospheric and Solar-Terrestrial Physics 63, 1661–1680.

Torr, M.R., Torr, D.G., 1973. The seasonal behaviour of the F2-layer of the ionosphere. Journal of Atmospheric and Solar-Terrestrial Physics 35, 2237–2251.

Wills, D.M., Hewish, A., Rishbeth, H., Rycroft, M.J., 1994. Synoptic data for solar-terrestrial physics: the UK contribution to long-term monitoring. Journal of Atmospheric and Solar-Terrestrial Physics 56, 871–886.

Wright, J.W., 1963. The F region seasonal anomaly. Journal of Geophysical Research 68, 4379–4381.

Yonezawa, T., Arima, Y., 1959. On the seasonal and non-seasonal annual variations and the semi-annual variation in the noon and midnight electron densities of the F2 layer in the middle latitudes. Journal of Radiology Research Labss 6, 293–309.

Yonezawa, T., 1971. The solar-activity and latitudinal characteristics of the seasonal, non-seasonal and semi-annual variations in the peak electron densities of the F2-layer at noon and midnight in the middle and low latitudes. Journal of Atmospheric and Solar-Terrestrial Physics 33, 889–907.

Zou, L., Rishbeth, H., Muller-Wodarg, I.C.F., Aylward, A.D., Millward, G.H., Fuller-Rowell, T.J., Idenden, D.W., Moffett, R.J., 2000. Annual and semiannual variations in the ionospheric F2-layer: I. Modelling. Annales Geophysicae 18, 927–944.